

Denoising spinal cord fMRI data: approaches to acquisition and analysis

Falk Eippert^a, Yazhuo Kong^a, Mark Jenkinson^a, Irene Tracey^a, and Jonathan C.W. Brooks^b

^a Oxford Centre for Functional Magnetic Resonance Imaging of the Brain, Nuffield Department of Clinical Neurosciences, University of Oxford, Oxford, UK

^b Clinical Research and Imaging Centre, University of Bristol, Bristol, UK

Corresponding author:

Dr. Jonathan Brooks

Clinical Research and Imaging Centre, University of Bristol

60 St Michael's Hill

BS2 8DX Bristol

United Kingdom

Phone: +44 117 342 1512 / Email: jon.brooks@bristol.ac.uk

Abstract

Functional magnetic resonance imaging (fMRI) of the human spinal cord is a difficult endeavour due to the cord's small cross-sectional diameter, signal drop-out as well as image distortion due to magnetic field inhomogeneity, and the confounding influence of physiological noise from cardiac and respiratory sources. Nevertheless, there is great interest in spinal fMRI due to the spinal cord's role as the principal sensorimotor interface between the brain and the body and its involvement in a variety of sensory and motor pathologies. In this review, we give an overview of the various methods that have been used to address the technical challenges in spinal fMRI, with a focus on reducing the impact of physiological noise. We start out by describing acquisition methods that have been tailored to the special needs of spinal cord fMRI and aim to increase the signal-to-noise ratio and reduce distortion in obtained images. Following this, we concentrate on image processing and analysis approaches that address the detrimental effects of noise. While these include variations of standard pre-processing methods such as motion correction and spatial filtering, the main focus lies on denoising techniques that can be applied to task-based as well as resting-state data sets. We review both model-based approaches that rely on externally acquired respiratory and cardiac signals as well as data-driven approaches that estimate and correct for noise using the data themselves. We conclude with an outlook on techniques that have been successfully applied for noise reduction in brain imaging and whose use might be beneficial for fMRI of the human spinal cord.

1. Introduction

Functional magnetic resonance imaging (fMRI) of the spinal cord is still at a relatively early stage. While the first reports of spinal fMRI appeared in the late 1990s (human imaging: Stroman et al., 1999; Yoshizawa et al., 1996; animal imaging: Pórszász et al., 1997), the field is still relatively small – there are currently about 100 published reports in humans and less than 50 in animals on spinal imaging with fMRI. In this review we will solely focus on the human spinal imaging literature, although exciting advances have been made with regard to spinal imaging in rats (e.g. Lawrence et al., 2004; Lilja et al., 2006; Zhao et al., 2009), cats (Cohen-Adad et al., 2009a), and very recently also in monkeys (Chen et al., 2015; Yang et al., 2015), where fine-grained sensory processing patterns were investigated as well as changes in resting-state connectivity due to spinal cord injury. It will be exciting to see how these approaches develop, especially when considering their application in tandem with other techniques such as two-photon imaging (Johanssen & Helmchen, 2013) or optogenetics (Montgomery et al., 2016).

A likely reason for the relative dearth of spinal fMRI studies lies in the difficulty of obtaining reliable results from this structure, which is due to a number of factors (Giove et al., 2004; Stroman, 2005; Stroman et al., 2014; Summers et al., 2010). First of all, the spinal cord has a very small cross-sectional diameter (approximately 12mm in the left-right and 8mm in the anterior-posterior direction at the cervical level; Fradet et al., 2014; Ko et al., 2004), which makes it necessary to use a high in-plane resolution to minimize partial-volume effects. Second, the presence of tissue-types with different magnetic susceptibility (vertebrae and connective tissue) leads to inhomogeneities in the static magnetic field (B_0) that result in a periodic signal disruption along the superior-inferior axis of the spinal cord (Cooke et al., 2004; Finsterbusch et al., 2012). Third, the influence of physiological noise (arising from respiratory and cardiovascular sources; Figure 1) on blood-oxygen-level-dependent (BOLD) responses is much stronger in the spinal cord than in the brain (Cohen-Adad et al., 2010; Piché et al., 2009), with the potential for obscuring task-related responses and resting-state connectivity profiles, unless adequately addressed.

With regards to the sources of physiological noise, one can dissociate respiratory and cardiac influences (though interactions are also observed; Brooks et al., 2008). Respiratory influences are mostly evident in time-dependent distortions of the B_0 field time-locked to the respiratory cycle (Raj et al., 2001) – these manifest as apparent non-rigid motion of the spinal cord and are much stronger than in the brain due to the spinal cord's proximity to the lungs (Verma and Cohen-Adad, 2014). Cardiac influences manifest themselves in vascular pulsations (Dagli et al., 1999) on the one hand, which might obscure spinal cord BOLD responses since the main arteries and veins run directly along the edge of the cord in close proximity to the minute grey matter regions of interest (Cohen-Adad et al., 2010). On the other hand, cardiac activity leads to pulsatile movement of the cerebrospinal fluid (CSF; O'Connell, 1943)

in which the spinal cord is embedded, resulting in a non-rigid oscillatory cord motion time-locked to the cardiac cycle (Figley and Stroman, 2007). Cardiac induced CSF-flow furthermore leads to large signal variations due to unsaturated spins moving into an imaging slice (Finsterbusch et al., 2012), which is highly problematic considering the proximity of the CSF-containing subarachnoid space to the spinal cord grey matter.

In spite of all these difficulties, there is great interest in studying the human spinal cord non-invasively, since it is the brain's principal sensorimotor interface with the body – thus properly characterising input to and output from the central nervous system relies on knowledge of spinal cord activity. Furthermore, there is also strong clinical interest in the spinal cord, due to its prominent involvement in a number of neurological disorders (Wheeler-Kingshott et al., 2014). For example, in multiple sclerosis, deficits in motor function may be due to dysfunction at multiple levels of the neuro-axis, and early spinal cord involvement in the primary progressive form of the disease has recently been demonstrated (Abdel-Aziz et al., 2015). Equally, damage occurring to motor neurons in amyotrophic lateral sclerosis have been shown to involve both the cortico-spinal tract and the spinal cord (Foerster et al., 2013). In patients with spinal cord injury the motivation to study the cord is clear and current interest includes relating cord atrophy to disability and monitoring treatment success (Cadotte and Fehlings, 2013; Freund et al., 2013), though imaging presents unique challenges due to the use of metal in stabilising the vertebral column. Lastly, the development and maintenance of chronic pain states in animal models has been shown to depend on altered spinal cord function (Woolf and Salter, 2000) and spinal cord fMRI would allow researchers to examine whether similar changes underlie the transition to chronic pain in man.

Here we set out to give an overview of approaches that have been used to overcome some of the aforementioned problems. We will first look at how one can optimise the signal-to-noise ratio (SNR) during image acquisition, based on a variety of methods that might not necessarily be routinely used in brain imaging. Then we will move on to describe the analysis approaches that have been developed to deal with the various sources of noise present in spinal fMRI data – here we will also mention differences when denoising task-based versus resting-state data. We will briefly mention various motion correction and spatial filtering approaches before concentrating on the main topic of denoising using either modelling approaches based on externally acquired signals (cardiac and respiratory data) or data-driven approaches that aim to find structured noise in the data that is then used in clean-up procedures. We will conclude with an outlook on procedures that have proven helpful for denoising brain fMRI data and might hold potential for spinal fMRI as well.

2. Acquisition approaches to denoising

Before coming to acquisition methods that optimize the SNR in the spinal cord, it is important to briefly review the gross anatomy and vascular supply of the spinal cord (Baron, 2015; Silverdale, 2015; Thron, 2016). From the superior to inferior (rostral to caudal) direction, the spinal cord is organized into cervical, thoracic, lumbar, sacral, and coccygeal parts; hereafter we will focus on studies of the cervical spinal cord as this part has received the greatest attention. Each of these parts contains several segments (31 in total) that correspond to left and right pairs of spinal nerves innervating a specific body territory. Sensory nerves enter the spinal cord on the posterior (dorsal) side and synapse mostly within dorsal grey matter, whereas motor nerves leave the spinal cord on the anterior (ventral) side, originating from ventral grey matter. The internal structure of the cord is best described as four grey matter horns that are embedded within the white matter tracts that provide connections between the spinal cord and the brain, as well as between spinal cord segments. Somatosensory (and viscerosensory) processing occurs mainly in the dorsal horns, whereas the processing and relay of motor commands to the muscles is a function of the ventral horns; autonomic processing occurs in the lateral column that is however not present throughout the cord's rostro-caudal extent. The spinal cord is supplied with blood via the anterior spinal artery and the posterior spinal arteries that run along the cord and give rise to a dense array of capillaries penetrating the cord. There is a roughly similar arrangement of draining veins that exit the cord to form a network with larger veins that run along the cord. When using blood flow sensitive measurements such as BOLD-based fMRI to infer neuronal activity, alterations to vascular tone (e.g. vasodilation due to increased CO₂ concentration in the blood) may become important. Notably, the effect of resting fluctuations in end-tidal CO₂ has been detected in brain fMRI data (Wise et al., 2004), and experimental manipulation of end-tidal CO₂ levels (i.e. hypercapnia) has been used to investigate vascular responses in the human spinal cord (Cohen-Adad et al., 2010).

When attempting to measure BOLD signal changes from the human spinal cord every effort should be made to optimize data acquisition as far as possible, and we will highlight several possibilities here. As with all MRI, the uniformity of the magnetic field in and around the structure of interest has a large influence on the quality of imaging data acquired. Scanner manufacturers routinely include an option to adjust the static magnetic field around a user-selected region of interest (volume shimming), to make the magnetic field as homogeneous as possible – such an approach should always be employed as a first step, no matter which kind of protocol one chooses to acquire spinal fMRI data. When choosing the target volume for the shim adjustment (usually a rectangle centred on the spinal cord), it should be kept in mind that a minimum size is required for the shim algorithm to work properly and that focussing the shim adjustments on the target region will lead to reduction in image quality in other parts of the image (Finsterbusch, 2014).

A further issue that is relevant for all of imaging, but particularly so for spinal fMRI, is movement of the structure of interest. The attribution of signal change to altered blood flow and volume (in the case of BOLD functional imaging), rather than to movement, is key to determining the “true” response of the system. Several approaches to minimizing cord movement have been taken, and one of the first used was cardiac gating, which attempts to capture images at the quiescent period of the cardiac cycle, when the cord is relatively still (Summers et al., 2006). One significant problem with this approach is that unless corrected for, gating will introduce a signal dependency on the cardiac cycle, as the time between samples is no longer governed by the scanner repetition time (TR), but by heart rate instead. The induced signal fluctuation is primarily due to different amounts of T_1 relaxation occurring between acquisition of image volumes (Huettel et al., 2014). Whilst, in principle, it should be possible to correct for the heart rate/ T_1 interaction, the correction relies heavily on perfect motion correction, and knowledge of the T_1 relaxation rate of the structure of interest (Guimaraes et al., 1998; Malinen et al., 2006). A further problem in the context of task-based acquisitions is the possibility that the experimental stimulation might systematically alter heart rate, meaning that correction has its greatest effect during stimulation, potentially introducing correction-dependent artefacts. Lastly, movement of structures within the field of view, but outside the structure of interest, may cause noise within the cord. In particular, movement of the jaw, larynx (through swallowing) or chest wall may all induce signal fluctuations that are “smeared” across the phase-encoding direction (Zhang et al., 2009). One approach to minimising such effects is to use saturation pulses to suppress signal from areas outside the cord (Wilm et al., 2007). Unfortunately, these pulses rarely suppress signal perfectly, they increase the amount of radiofrequency energy deposited in the body, and each applied saturation band reduces the time available for data acquisition (reducing the number of slices per TR).

Of particular importance when acquiring functional data from the spinal cord is the ability to resolve small areas of activity that can, at the coarsest level, be assigned to quadrants of the cord – heuristically, this will at least make it possible to distinguish sensory and motor processes as well as their laterality. Given the small size of the cord, this necessitates the use of relatively small voxels. When imaging the cord in the axial plane, one would typically use small voxels, i.e. a high in-plane resolution (e.g. 1x1mm voxel size in x and y direction) combined with a large slice thickness (e.g. 5mm voxel size in z direction). The consequences of this choice are 1) low inherent SNR (proportional to the volume of each voxel), 2) signal loss due to intra-voxel dephasing (caused by magnetic field variation through the slice, particularly affecting gradient echo acquisitions such as echo planar imaging), and 3) image distortion due to off-resonance effects (caused by magnetic field variation primarily in the low bandwidth phase encoding direction).

The first of these issues can be mitigated to a certain extent a) by improving receive coil design (Cohen-Adad and Wald, 2014) to maximize the amount of recorded signal, b) by increasing voxel size (at the expense of tissue specificity), or c) by lengthening

the acquisition (increased averaging). One possible solution to the second issue of intra-voxel dephasing would seem to be to reduce the slice thickness, at the expense of a further decrease in SNR. Whilst it may seem counterintuitive to use relatively thick slices, this actually capitalizes on the anatomical arrangement of the spinal cord, which has a laminar arrangement with layers of similar cells stacked longitudinally in the cord, thus increasing the chance of signal detection by sampling from a larger pool of similar neurons. An alternative and elegant solution to this problem is to adjust the main magnetic field on a slice by slice basis during acquisition, to “shim” away the through slice variation in B_0 field. This slice-specific z-shimming approach (Finsterbusch et al., 2012) leads to a drastic reduction in signal intensity variation along the cord (of about 80%) by reducing the periodically occurring signal drop-outs. This technique thus protects against an excess of false negatives that could arise from signal loss in regions of interest. The third issue, image distortion (Figure 2), is particularly problematic with single-shot techniques that employ a relatively large matrix size (necessary to capture the fine detail in the cord) and a large field of view (necessary to avoid signal aliasing or “phase-wrap”). This combination leads to a large amount of time required to fill k-space (read-out duration), with a corresponding increase in time to acquire each line of k-space (echo-spacing). The net effect of this is to produce blurring in the image, and image distortion in the phase-encode direction, where signal is mislocated. There are several different approaches to mitigate these problems, and these are reviewed in detail elsewhere (Saritas et al., 2014). Briefly, these techniques all seek to minimize the amount of time taken to fill k-space, and they achieve this either through the use of parallel imaging techniques such as GRAPPA or SENSE (Griswold et al., 2002; Pruessmann et al., 1999), multi-shot gradient echo acquisitions (Barry et al., 2011), or by selectively exciting an inner field-of-view to minimize the number of k-space lines required whilst avoiding phase-wrap (Finsterbusch, 2013; for a recent spinal fMRI application see Weber et al., 2016).

When considering whether modifications to acquisition have actually improved data quality, a useful measure to consider is the temporal SNR (tSNR; Parrish et al., 2000). Normally estimated from resting fMRI data, tSNR is calculated by taking the ratio of the temporal mean to the temporal standard deviation of time series data following motion correction. As an aside, motion correction normally employs trilinear or spline-based interpolation, the former of which typically introduces substantially increased spatial smoothness in the data. For the purpose of assessing tSNR one can use nearest neighbour interpolation (which will not induce extra smoothness but may leave in some residual movement effects) or spline-based interpolation (which will induce a very small amount of extra smoothness) to minimise bias in the tSNR estimates. Areas with high intrinsic mean signal and low signal variation will give rise to large tSNR values, which is a useful measure when considering whether it will be possible to distinguish neuronally induced signal from noise (Cohen-Adad et al., 2010). In addition to tSNR, one might also want to investigate changes in functional contrast-to-noise ratio (CNR; Welvaert & Rosseel, 2013).

In the next section of this review we will cover analysis approaches to noise reduction, which can be quite effective. It needs to be stressed however, that due to the difficulties spinal fMRI faces (small cord diameter, signal dropout and distortion due to field inhomogeneities, impact of physiological noise) it is absolutely essential that steps are taken at the acquisition stage to mitigate sources of noise – otherwise the obtained data might be seriously compromised.

3. Analysis approaches to denoising

3.1 Data inspection and motion correction

A crucial first step to analysing spinal fMRI data is visual inspection of the recorded time series data – this might highlight problems such as large movements (e.g. induced by swallowing) or increases in background noise (e.g. ghosting) that affect discrete volumes. In these situations, there are several approaches to deal with the affected volumes, such as replacing the affected volumes by the average of its neighbours, replacing the affected volumes by the time-series average, using regression models that essentially remove the artefactual effects from the data or simply (in the case of resting-state data) deleting the affected volumes from the time-series; this is currently a very active field of research that is described in detail elsewhere (Power et al., 2015; Pruim et al., 2015a).

One source of apparent movement seen when looping through fMRI time series of axially acquired spinal cord data, is an oscillation in the phase encoding direction. The source of this apparent movement is the respiratory cycle (Verma and Cohen-Adad, 2014), which introduces breathing dependent shifts in the B_0 field that translate to image shifts in the phase-encode direction. Indeed, power spectra computed from the time-series of motion amplitudes in the phase-encode direction will typically demonstrate a peak at around $\sim 0.3\text{Hz}$ indicating a respiratory influence on cord motion. It should be noted that conventional methods for motion correction, which assume that movement can be characterized by rigid body transformations (Jenkinson et al., 2002), may not be sufficient to correct for differing amounts of movement along the cord due to spatial variation in B_0 and effects such as swallowing. To address these problems researchers have tended to adopt motion correction techniques that work on a slice-wise basis, and appear to be more appropriate (Cohen-Adad et al., 2009b; Weber et al., 2014). These techniques will usually restrict correction to two degrees of freedom, adjusting for in-plane translations (x and y), ignoring translations in, and rotations about, the z (i.e. slice) direction (Brooks et al., 2008; Brooks et al., 2012). While theoretically motivated, the slice-wise motion correction approach sometimes lacks robustness, and developments are underway to correct for this by imposing a certain amount of regularisation along the z-direction (Cohen-Adad et al., 2015).

3.2 Spatial and temporal filtering

Further processing steps that aim to reduce noise and thereby increase the tSNR of the recorded data are spatial and temporal filtering of the data. The aim of spatial smoothing, which behaves like a spatial low-pass filter, is to remove ‘speckled’ high-frequency noise and increase SNR. While the use of an isotropic three-dimensional Gaussian kernel – often with a full width at half-maximum of at least twice the voxel size – is a standard procedure in fMRI of the brain for a number of reasons (e.g. to

reduce noise in the image, to reduce the effects of inter-individual differences in anatomy, to ensure that the data conform to the assumptions of Gaussian random field theory), it should be used with caution in spinal cord fMRI. First, since the grey matter – especially at the tip of the dorsal horns – immediately borders areas of high signal variation (CSF space), isotropic smoothing is likely to introduce high-intensity noise that might swamp subtler signals from grey matter. Second, the anatomical organization of the spinal cord – with narrow dorsal horns enclosed on both sides by white matter – does not lend itself well to isotropic smoothing, as it will introduce strong partial volume effects between the grey and white matter.

An alternative approach is to use an anisotropic smoothing kernel, with minimal smoothing in the x and y directions, but much stronger smoothing in the z-direction. The benefit of this approach is that it will lead to an increase in SNR, but will only introduce small contributions from white matter and CSF signals – furthermore, it is unlikely that this approach leads to a loss in spatial specificity along the cord, since each spinal segment (i.e. the unit of anatomical resolution currently investigated) has an extent of about 15mm in the rostro-caudal direction (Ko et al., 2004). A finessed version of this approach (Cohen-Adad et al., 2014) uses a three-step procedure: first the spinal cord is straightened along its centerline, then smoothing is applied only along the rostro-caudal axis, and then the smoothed cord is de-straightened, i.e. brought back into its original position. This procedure has the obvious advantage over basic anisotropic smoothing in that it virtually eliminates the possibility that CSF signal will be introduced into the grey matter due to the cord curvature. A final – and very different – approach does not use a local smoothing kernel (where a voxel value is replaced by a weighted average of its neighbours' values), but instead makes use of redundant information in the image (a voxel value is replaced by an average of voxels with a similar intensity and a similar neighbourhood structure). This so-called 'non-local means' filtering approach (Buades et al., 2005) has become popular in image processing and extensions have been developed in order to denoise structural MRI images (Coupe et al., 2008; Manjón et al., 2010). Due to its edge-preserving characteristics, it could also be a valuable approach for spinal cord fMRI data and initial results from fMRI data of small subcortical structures are encouraging (Bernier et al., 2014), though this clearly warrants more extensive validation, as it is likely that the temporal changes in the non-local regions are not related to the local effects of interest and therefore it is unclear how robust this technique would be.

When considering the frequency components within fMRI data, it is apparent that there is a reciprocal relationship between signal power and frequency, i.e. the $1/f$ noise characteristic (Zarahn et al., 1997). This becomes important when using parametric statistics for inference, as the underlying assumption is that the noise in the measurement is independent and identically distributed (iid), implying that there is an equal contribution of noise across the frequency spectrum (Purdon and Weisskoff, 1998). Several techniques exist for correcting for the influence of non-white noise in fMRI data based on pre-colouring (imposing a known correlation structure by low-pass filtering) or pre-whitening (estimating and removing the correlation structure);

generally, the latter method is now the preferred choice (Poldrack et al., 2011). The pre-whitening approach (the benefits of which for spinal fMRI have been demonstrated by Kong et al., 2012) is combined with high-pass filtering, which will help reduce the influence of slow drifts in signal intensity affecting the low frequency part of the spectrum and is a standard approach in task-based fMRI. Conversely, the use of low-pass or band-pass filtering outside of the general linear model, without explicit correction for this filtering, is not recommended (Brooks, 2014), as this will inevitably inflate false-positive rates by removing noise from the time series data prior to model estimation, leading to underestimation of residuals (artificially increasing confidence in estimated activity) in fixed-effects or mixed-effects analyses (Figure 3). When attempting to assess data quality following filtering, one should therefore be wary of basing decisions solely on increased tSNR, as apparent enhancements (e.g. by removing high frequency noise) may not translate to genuine improvement in signal detection (e.g., due to poorer estimates of the residual noise).

3.3 Modelling-based approaches to physiological noise correction

The purpose of fMRI analysis in a task-based setting is to attribute the recorded signal change to the employed paradigm, and this is conventionally done through first level analysis within the general linear model (GLM). To achieve this, one supplies a model that attempts to explain signal change within the experiment, e.g. by supplying a timing file that describes the onset and duration of an externally applied stimulus, which the GLM uses to estimate what portion of the signal can be uniquely assigned to the supplied regressor(s). The confidence in the estimated parameters (beta values), is dependent on the how large the effect is compared to the background variation in measured signal (the noise) and how many measurements were taken, and is used to calculate a t-, or Z-score with associated p-value. The noise estimate is taken to be the standard deviation of the residuals, i.e. the un-modelled signal that is left after model fitting. Areas such as the spinal cord and brainstem suffer from large noise contributions, primarily due to cardiac and respiratory processes (Bosma and Stroman, 2014; Brooks et al., 2008; Figley and Stroman, 2007; Kong et al., 2012; Piché et al., 2009; Verma and Cohen-Adad, 2014; for reviews, see Brooks, 2014; Fratini et al., 2013), which if left un-modelled will lead to increased variance in the residuals and consequently reduce confidence, or even invalid inference, in estimated activation parameters. Indeed, their contribution may mask the detection of signal if they share variance with the applied paradigm, leading to incorrect estimates of effect size. Fortunately, these physiological processes can be sampled relatively easily during scanning using electrocardiogram (ECG) leads or a pulse-oximeter for the cardiac waveform, and respiratory belt to measure respiratory effort (Figure 4a). Typically, these physiological waveforms can be logged along with scanner triggers (to relate these processes to the image acquisition) on either an analog-to-digital converter connected to a personal computer, or on the scanner's host computer. The goal of physiological noise correction is thus to take some measurement from the

participant, which could be an independent measure like cardiac or respiratory waveform or a derived measure taken from the data itself, like white matter signal, and remove this signal contribution from the time series. In this section we focus on physiological noise correction that is based on independent measures (the use of derived measures will be the topic of section 3.4). The approach originates from work by Glover and colleagues (Glover et al., 2000; often referred to as RETROICOR) and has been refined and applied to the spinal cord (Brooks et al., 2008; Kong et al., 2012; often referred to as PNM).

When dealing with independent measures these are typically used as inputs to a model that attempts to explain physiological signals that are present in recorded data e.g. cardiac-induced signal change. The relevant information from quasi-periodic signals like cardiac and respiratory waveforms is the phase of the process at the time of image acquisition (for respiratory data, amplitude is important as well, see below), and is summarized in Figure 4b. The cardiac phase can be assigned on the basis of a fraction of the cardiac cycle running from 0 to 2π , whereas respiratory phase takes into account both the position in the cycle at image acquisition and the depth of each breath. Respiratory phase can be derived using a histogram equalized transfer function (Glover et al., 2000), that assigns values on the basis of the accumulated phase estimated from a histogram of all respiratory data, and runs from $-\pi$ to $+\pi$, where the sign indicates whether the image was acquired on the inspiratory or expiratory portion of the cycle (Figure 4b). The estimated cardiac and respiratory phase is then fed into a Fourier basis set consisting of a series of sine and cosine terms and their interaction (Brooks et al., 2008), whose purpose is to approximate physiologically induced signal change in fMRI data by generating new explanatory time-series regressors. There are two quite distinct options with how to proceed with these regressors: one approach applies them to the k-space time-series data to remove global physiological effects from the data (Hu et al., 1995; RETROKCOR), whereas the other approach, which we focus on here, applies them to the time-series in image space (Glover et al., 2000; RETROICOR). When working with image data there are broadly two options for how to correct for physiological signals: i) pre-filtering prior to model estimation with the GLM, and ii) model estimation including physiological regressors within the GLM. We will focus on the second of these options first. Please note that this is not an exhaustive description of the many different physiological noise modelling techniques that have been described and implemented across different software packages.

When a physiological model is included within the GLM, the amplitudes (beta value of parameter estimate) of the regressors from the Fourier basis-set used to model the physiological signals are adjusted by the GLM to optimally fit the time series data alongside the explanatory regressor(s) that describe task related activity. As such, modelling within the GLM automatically adjusts for loss of degrees of freedom and provides an accurate and convenient method for correcting for physiological effects. Regarding the estimated effect sizes provided by the GLM, the variance estimate associated with each parameter of interest derives from the residuals after

modelling with the GLM (in FSL, this is the “varcope” image). If residuals are artificially smooth, as will occur when pre-filtering prior to model estimation, the variance associated with each regressor of interest can be under-estimated if not explicitly accounted for (as noise has already been removed). When assessing group activity using first-level results from data that were pre-filtered outside the GLM, e.g. counting the number of activated voxels within the cord, results may be biased due to inflation of false positives. Similarly, when passing data up for group analysis, particularly when using parametric mixed effects modelling (which uses information on the variance of individual participant’s parameter estimates), group effects can be over-estimated due to incorrect variance estimates at the first level. Pre-filtering outside of the GLM will still reduce the contribution from physiological noise, and can be used to clean up data prior to first-level model estimation, providing one intends to use ordinary least squares modelling (which is possible in all standard neuroimaging packages) or non-parametric permutation testing (which can be done with tools such as SnPM [<http://warwick.ac.uk/snpm>] within SPM or Randomise [<http://fsl.fmrib.ox.ac.uk/fsl/fslwiki/Randomise>] within FSL) for group level inference. Lastly, whilst not all analysis software currently offers the possibility of including slice-specific regressors at the first level, this should be addressed through future developments, as assigning cardiac phase based on a volume trigger will be inaccurate for most slices with typical repetition times.

Several alternative approaches to the above described modelling of physiological noise in spinal fMRI have been proposed. Stroman (Stroman, 2006) recorded peripheral pulse oximetry and respiratory belt data during functional imaging of the spinal cord, using a single shot fast spin-echo sequence. These traces were then down-sampled to the timing of each slice, and these aliased time courses further reduced by a principal component analysis (PCA) to produce a basis set. The final basis set was included along with the experimental timing of somatosensory stimulation in a GLM to estimate activation patterns. Intriguingly the amount of type-I errors, indicated by somatosensory stimulation-induced activity in bone and connective tissue (i.e. outside the cord), appeared to increase with inclusion of the cardiac and respiratory basis set – suggesting a failure to adequately account for these processes. Figley and Stroman later proposed a different approach for spin-echo data, in which they used principle components of anterior-posterior spinal cord motion (time-locked to the cardiac cycle; Figley and Stroman, 2007) as regressors in a GLM analysis and showed improved sensitivity and specificity (Figley and Stroman, 2009). As a further alternative, it may be possible to use a finite impulse response function approach to model physiological noise (Deckers et al., 2006). In this denoising technique, the cardiac and respiratory cycles are arbitrarily divided up into discrete equally spaced intervals (or bins), and each image slice assigned to one of the cardiac and respiratory bins on the basis of their acquisition time. By re-ordering data according to bin membership and averaging responses within each one, it is possible to approximate the cardiac and respiratory effects at each time-point, which are then removed from the original data. This approach is model-free, in that it has no assumed

shape for the induced physiological effect on the image data. However, it cannot adjust to different depths of breathing and may be problematic to include within the framework of the GLM unless slice-specific regressors can be specified. In an evaluation study (Kong et al., 2012) it has also been shown to be outperformed by the above-mentioned extended RETROICOR model (PNM).

3.4 Data-driven approaches to physiological noise correction

The previously described denoising methods rely on the acquisition of additional external signals, such as respiratory and cardiac waveforms, and in some circumstances a model that explains how their effects relate to the fMRI data. However, it is also possible to denoise fMRI data using methods that rely on the fMRI data themselves to construct noise regressors. Such data-driven methods have the obvious advantage that they do not require recording of additional signals and they also do not make any specific assumptions on how externally acquired signals should be modelled (e.g. by sine and cosine terms as in RETROICOR). However, it is worth noting that there is a risk of removing signals of interest i.e. those associated with the experimental paradigm, so care should be taken when identifying noise sources. Please also note that our aim is not to review every possible data-driven noise-reduction method developed for fMRI of the brain – instead we choose to focus on two approaches that have already been applied to the spinal cord.

One example is the CompCor method (Behzadi et al., 2007; Muschelli et al., 2014) that derives noise regressors from regions that are unlikely to contain neuronal signals, but whose signals will be driven by structured noise, which will similarly affect – and thus adequately model physiological noise in – the grey matter. In the brain this approach entails choosing noise ROIs either on anatomical grounds (e.g. using white matter and ventricle ROIs based on segmentation) or on the temporal standard-deviation of time-series (where a high standard deviation has been shown to be driven by physiological noise). One then uses PCA to obtain characteristic representations of the physiological fluctuations in the noise ROIs and uses these time-courses as covariates in a GLM analysis. It is important to point out that by extracting a number of principal components per noise ROI, this approach allows several distinct noise processes to exist in the same ROI, which makes it superior to denoising methods that rely on the average signal of noise ROIs (where the averaging procedure might actually lead to cancelling out of disparate noise signals; Muschelli et al., 2014). This approach has been shown a) to significantly reduce the temporal standard deviation of resting-state data, b) to significantly increase the number of activated voxels in task-based data, and c) to outperform RETROICOR-based denoising (Behzadi et al., 2007).

Barry and colleagues (2014, 2016) successfully used this approach in their spinal cord resting-state studies at 7 Tesla, where they obtained distinct and reproducible time-course correlations between dorsal horns and between ventral horns. Interestingly, they applied several CompCor steps in succession, with denoising based on principal

components obtained from the non-spinal part of the image being carried out before motion correction, and denoising based on principal components obtained from white matter and CSF being carried out after motion correction and physiological noise regression using RETROICOR. This sequence of processing steps optimised the combined effects of these procedures and worked well at lower field strength too (Barry, personal communication), so it will be interesting to formally test whether this might indeed be the optimal sequence of denoising steps at every field strength (Jones et al., 2008), since the influence of physiological noise varies with field strength (Triantafyllou et al., 2005). It is also important to note that extracting several components from the CSF surrounding the spinal cord is potentially a sensible approach, because CSF flow is not homogeneous but is instead organized into distinct channels with different time-profiles (Henry-Feugeas et al., 2000; Schroth and Klose, 1992).

There are however a few caveats when using a CompCor-based approach to perform data-driven denoising in spinal fMRI. First, one needs to make sure that the acquisition parameters are chosen such that ghosting is minimized (see Finsterbusch et al., 2012 for an example), as one might otherwise remove signal of interest when deriving components from a non-spinal region. Second, the close proximity of the CSF-containing subarachnoid space to the grey matter of the spinal cord makes it possible that one actually removes signal of interest. This issue is particularly pronounced for the dorsal horns, which almost extend to the edge of the spinal cord – with the current spatial resolution achievable at 3T this will invariably lead to signal-mixing. To alleviate this, one could either construct an eroded ROI that does not include cord-edge / CSF voxels, or in the case of task-based fMRI one could exclude voxels that show a significant correlation with the paradigm (Behzadi et al., 2007) or orthogonalise the obtained CSF regressors to the paradigm (Brooks et al., 2012). Third, using the WM as a noise ROI for component extraction might be sensible at 7T where a higher spatial resolution and a smaller point-spread function (Shmuel et al., 2007) will mitigate partial volume effects and signal mixing. At 3T however, a PCA based on white-matter voxels will most likely produce components that contain signal of interest. Furthermore, the distortion that is present in gradient-echo EPI images will also limit an accurate delineation of a white-matter ROI – but with the current development of tissue-type segmentation and incorporation of this information into registration procedures, this latter concern might be alleviated in the future (Asman et al., 2014).

Another data-driven approach to denoising that has been applied to spinal fMRI data is CORSICA (Perlberg et al., 2007) – CORrection of Structured noise using Spatial Independent Component Analysis. It is based on decomposing the data into a set of spatial components and associated time-courses (via spatial independent component analysis; see below and Beckmann, 2012), identifying noise components based on the similarity of their time-courses to time-courses obtained from noise masks (using a rather elaborate procedure), and then removing their influence by reconstructing the data using all components except those identified to represent noise. The benefit of this approach is that it can be applied to data acquired with a standard TR, since it is

based on spatial priors for identifying components as noise, whereas previous studies identified noise components based on their spectral profile – high power at the cardiac and respiratory frequencies – which necessitates a very short TR for acquisition to avoid aliasing. A slightly modified version of this approach has recently been used to demonstrate that it can be beneficial in detecting pain-related responses in the spinal cord (Xie et al., 2012). In addition to fMRI data used to investigate pain-related responses – which were acquired with a standard TR – these authors also acquired short-TR data for each participant, which were used to generate participant-specific noise maps based on spatial independent component analysis (where noise components were identified by calculating spectral coherence between the component time-courses and cardiac and respiratory data). Using the standard CORSICA approach with these noise maps resulted in reduced high-frequency variation in the time-series and a higher number of significant voxels as well as mean t-scores in the cord, but not in the subarachnoid space, arguing for the spatial specificity of this technique. One critical difference to the original CORSICA approach is that the authors did not choose the noise maps based on spatial priors, but instead based them on an ICA of the short-TR data in combination with cardiac and respiratory signals – while this an important step for method validation, it will arguably be important to be able to use CORSICA without such need for additional data acquisition.

Finally, the masked-ICA approach (Beissner et al., 2014; Moher Alsady et al., 2016) that has been validated in the brainstem should be mentioned as well. This technique is only applicable to situations where one wishes to use ICA-based data analysis and reduces the impact of physiological noise by excluding regions with high noise levels from the volume of interest in which an ICA is performed. Kong et al. (2014) used this approach when investigating spinal cord resting-state fluctuations via ICA – however, since comprehensive physiological noise modelling was employed at the same time, it was not possible to judge the isolated effect of the masked ICA approach.

4. Outlook

In closing, we would like to highlight a few approaches that have shown beneficial effects for noise reduction in the brain. Since many of the problems that these approaches aim to ameliorate exist in the spinal cord to a larger degree, their application to spinal fMRI might be of significant benefit.

4.1 Acquisition

A major concern when imaging the spinal cord is the contribution from CSF affecting signal measured in the cord (Kong et al., 2012). A recently developed pulse sequence offers the possibility of minimising contributions from inflowing CSF signal, whilst leaving static tissues unaffected (Li et al., 2012). This so-called DANTE-EPI sequence achieves suppression of flowing CSF spins through repeated application of non-selective low flip-angle excitation in the presence of gradient pulses, and should help to improve tSNR of spinal EPI data, and hence signal detection. It should be noted that it is also possible to suppress flow through the use of inversion recovery techniques or diffusion-weighting gradients (Andersson et al., 2002) – such flow compensation techniques have been extensively applied in spinal fMRI (Bouwman et al., 2008; see also Finsterbusch et al., 2012) and it will be interesting to see how their benefits compare to those obtained by using DANTE-EPI. An alternative approach to correcting for physiological artefacts is to acquire additional images that sample these processes at the time of acquisition and use that information to subtract their effects from BOLD-sensitive EPI data. These multi-echo functional imaging techniques (Kundu et al., 2012) have shown great promise for improving the quality of fMRI data acquired from the brain, but have yet to be exploited for imaging the spinal cord. One might also use simultaneous multi-slice (or “multi-band”) EPI, which allows a shortening of the TR due to the simultaneous excitation of several slices (Barth et al., 2016; interestingly, this approach has recently been combined with a multi-echo technique: Boyacioğlu et al., 2015); this approach requires a certain coil geometry, but would potentially allow one to critically sample cardiac and respiratory artefacts and thus remove them based on frequency spectra (which is not possible with standard TRs due to the aliasing that occurs). An alternative approach to improving the specificity of spinal cord fMRI is to reduce voxel sizes, which has been shown to reduce the influence of physiological noise (Hutton et al., 2011). In practise, this approach only becomes feasible when moving to higher field strengths such as 7T and above. Due to the lack of body coils at 7T, this has necessitated the development of novel transmit/receive coils for spinal cord applications (Zhao et al., 2014), the improvements from which are only now being realised. There are also possibilities to address the effects of magnetic field inhomogeneities evident in the neck region (due to the different susceptibilities of air and tissue), which make adequate shimming more difficult. These static B_0 inhomogeneities can be ameliorated by using a foam cushion around the neck that consists of tissue susceptibility matched pyrolytic graphite foam

(Lee et al., 2015), which should benefit gradient-echo EPI acquisitions. However, even if the static B_0 distortions can be compensated with such an approach, this still leaves dynamic B_0 distortions induced by breathing. Considering that these distortions can be of the same size as the cord's anterior-posterior diameter (Verma and Cohen-Adad, 2014), it would be very welcome to not only address the apparent cord movement by post-hoc procedures such as slice-wise motion correction, but to correct them prospectively. This could be realized through a dynamic compensation via real-time shim updating based on simultaneously acquired respiratory data – such an approach has been applied in the brain (van Gelderen et al., 2007), but as yet not in the spinal cord, where its effects are expected to be even more beneficial.

4.2 Analysis

Similar to the above-described acquisition methods, here we would like to highlight a few approaches with regards to denoising from the analysis perspective that have gained prominence in brain imaging, but have largely not been applied to spinal fMRI. These approaches are all based on independent component analysis or ICA, a blind source separation technique that allows multivariate data to be decomposed into a number of components. In the context of fMRI, spatial ICA decomposes the four-dimensional data into a set of three-dimensional independent component maps and associated time-courses (Beckmann, 2012). These components can either represent true signal (that is neurally generated), noise (from various sources) or a mixture of both. A typical data-driven denoising approach would thus consist of running an ICA, identifying noise components and then removing these from the data. The practical variability in ICA-denoising approaches mostly pertains to the second step, i.e. the identification of a component as noise – this can be done in a manual or an automated fashion and on the individual or group level.

The traditional – and easiest to implement – approach is to run a spatial ICA for each participant and to then carry out a manual classification of components into signal or noise. Guidelines for hand-classification of brain fMRI have been developed (Kelly et al., 2010; Griffanti et al., submitted), but may not be applicable to the spinal cord in their entirety. Nevertheless, a large number of features that indicate if components are noise will apply to the spinal cord as well (e.g. spatial overlap with vasculature, sudden jumps in time-series, strong high-frequency content in power spectrum). Once the components are identified, these can then be removed from the data (for task-based data, this should be done by including their time-courses as covariates in the design matrix). Such an approach has been taken in a recent resting-state spinal fMRI study (San Emeterio Nateras et al., 2016), as well as in a task-based study on motor-learning where the authors also explicitly listed their criteria for designating a component as noise (Vahdat et al., 2015). It is furthermore possible to combine ICA-based denoising with the model-based approaches described earlier; such an approach has recently been shown beneficial for brainstem data (Faull et al., 2016) and might hold potential for spinal fMRI as well.

Manual classification of components can also be performed at the group level, after running a group-level ICA analysis. This might be beneficial in cases where components are weak but consistent at the individual-participant level and will thus only become apparent at the group level. One can then use these group-level noise components and regress their three-dimensional spatial maps into each participant's four-dimensional fMRI data to obtain individual time-courses which can then be regressed out of each participant's four-dimensional fMRI data (inside the GLM for task-based data). To our knowledge, this technique of denoising via group-level component identification has not been carried out in any spinal fMRI study to date. As an aside, if one carries out a group-ICA on already denoised data (e.g. via physiological noise regression), this will allow one to judge how effective the used denoising procedure was: for example, in Kong et al. (2014), state-of-the-art physiological noise modelling was used (including cardiac and respiratory regressors with various harmonics, their interaction, motion parameters, changes in heart-rate, CSF signal), but at the group level distinct noise components could still be identified outside of the spinal cord. In any case, while a manual classification is straightforward to perform, it is time-consuming and incorporates a certain level of subjectivity.

To ameliorate these issues, a number of methods have been developed for automatic classification of components into signal or noise (for references, see e.g. Pruim et al., 2015b). Two of the most recent and already widely-used ones are FIX (FMRIB's ICA-based X-noiseifier; Salimi-Khorshidi et al., 2014) and ICA-AROMA (ICA-based strategy for Automatic Removal Of Motion Artefacts; Pruim et al., 2015b). FIX uses a large number of features (almost 200) and a combination of classifiers to identify components as signal or noise. This obviously makes it very flexible and thus sensitive to a large number of noise sources – however it also limits its generalizability, meaning that it needs to be retrained when a data-set differs from the data-sets on which FIX was trained. Applying the current implementation of FIX to the spinal cord is likely to be a major undertaking when considering that the large number of features were specifically chosen for fMRI of the brain.

ICA-AROMA on the other hand only uses four features (high-frequency content in component time-course, correlation of component time-course with estimated motion parameters, fraction of voxels of the component map that are at the edge of the brain, and fraction of voxels of the component map that are in the CSF-space) and a single classifier for component identification. Admittedly, ICA-AROMA was developed to solely deal with motion artefacts, but data suggest that it might also identify components as noise that reflect physiological noise processes. The current implementation of ICA-AROMA is only applicable to fMRI of the brain (since it makes heavy use of spatial features that rely on a standard space definition), but it is likely to be worthwhile applying a similar approach to denoising spinal cord data. Having access to an automated denoising tool might also lower the barrier for researchers to study the spinal cord, since the task of findings one's way through the labyrinth of denoising options and implementing one would be obsolete.

All the denoising methods discussed in this review are equally applicable to task-based and resting-state fMRI. However, a word of caution is necessary, since it is recommended that denoising regressors be included in the design matrix for task-based data analysis, as otherwise biased inference in a parametric mixed effects setting may occur at the group level – this is not an issue for resting-state analysis where other forms of inference are used. Nevertheless, several things should be kept in mind here as well. First, any kind of nuisance regression should be performed simultaneously with temporal filtering in order to avoid spectral misspecification (Hallquist et al., 2013). Performing it before temporal filtering is acceptable, but performing it after temporal filtering will lead to reintroduction of noise into the time-series and inflated correlations; if it is necessary for nuisance regression to be performed after temporal filtering, then one should apply the same filter to the nuisance regressors themselves. It is reassuring to see that previous spinal cord resting-state studies did not fall prey to this mistake when using nuisance regression (Barry et al., 2016, 2014; Kong et al., 2014). Second, the use of low-pass or band-pass filtering is questionable, as several recent brain imaging studies have shown that frequencies above the common cut-off of 0.1Hz do contain meaningful signal (e.g. Chen and Glover, 2015; Niazy et al., 2011). Within a limited frequency range, data from Barry and colleagues (2014, 2016) seem to suggest that this holds for the spinal cord as well. Third, accurate denoising is arguably even more important when using resting-state compared to task-based analyses (Murphy et al., 2013). Whereas the latter relate the data to an explicit model of the paradigm timing and use averaging to suppress task-unrelated noise, the former rely solely on correlations between voxel time-series that will be driven not only by neuronal factors but can also be affected by non-neuronal processes such as motion, scanner artefacts or physiological noise. Without appropriate denoising it is thus virtually impossible to link the observed functional connectivity results to a non-artefactual neuronal source – this is even more important for the spinal cord, where physiological noise is of greater magnitude than it is in the brain (Cohen-Adad et al., 2010; Piché et al., 2009).

In conclusion, we hope to have given an overview of denoising approaches for spinal fMRI, both on the level of data acquisition as well as data analysis. It should be borne in mind that denoising for fMRI data is a constantly evolving field, where current and future developments hold promise for significantly improving the reliability of spinal fMRI.

References

- Abdel-Aziz, K., Schneider, T., Solanky, B.S., Yiannakas, M.C., Altmann, D.R., Wheeler-Kingshott, C.A.M., Peters, A.L., Day, B.L., Thompson, A.J., Ciccarelli, O., 2015. Evidence for early neurodegeneration in the cervical cord of patients with primary progressive multiple sclerosis. *Brain* 138, 1568–1582. doi:10.1093/brain/awv086
- Andersson, L., Bolling, M., Wirestam, R., Holtås, S., Ståhlberg, F., 2002. Combined diffusion weighting and CSF suppression in functional MRI. *NMR Biomed.* 15, 235–240. doi:10.1002/nbm.767
- Asman, A.J., Bryan, F.W., Smith, S.A., Reich, D.S., Landman, B.A., 2014. Groupwise multi-atlas segmentation of the spinal cord's internal structure. *Med. Image Anal.* 18, 460–471. doi:10.1016/j.media.2014.01.003
- Baron, E.M., 2015. Spinal cord and spinal nerves: gross anatomy, in: Standring, S. (Ed.), *Gray's Anatomy: The Anatomical Basis of Clinical Practice*.
- Barry, R.L., Rogers, B.P., Conrad, B.N., Smith, S.A., Gore, J.C., 2016. Reproducibility of resting state spinal cord networks in healthy volunteers at 7 Tesla. *NeuroImage* 133, 31–40. doi:10.1016/j.neuroimage.2016.02.058
- Barry, R.L., Smith, S.A., Dula, A.N., Gore, J.C., 2014. Resting state functional connectivity in the human spinal cord. *eLife* 3, e02812.
- Barry, R.L., Strother, S.C., Gatenby, J.C., Gore, J.C., 2011. Data-driven optimization and evaluation of 2D EPI and 3D PRESTO for BOLD fMRI at 7 Tesla: I. Focal coverage. *NeuroImage* 55, 1034–1043. doi:10.1016/j.neuroimage.2010.12.086
- Barth, M., Breuer, F., Koopmans, P.J., Norris, D.G., Poser, B.A., 2016. Simultaneous multislice (SMS) imaging techniques. *Magn. Reson. Med.* 75, 63–81. doi:10.1002/mrm.25897
- Beckmann, C.F., 2012. Modelling with independent components. *NeuroImage* 62, 891–901. doi:10.1016/j.neuroimage.2012.02.020
- Behzadi, Y., Restom, K., Liau, J., Liu, T.T., 2007. A component based noise correction method (CompCor) for BOLD and perfusion based fMRI. *NeuroImage* 37, 90–101. doi:10.1016/j.neuroimage.2007.04.042
- Beissner, F., Schumann, A., Brunn, F., Eisenträger, D., Bär, K.-J., 2014. Advances in functional magnetic resonance imaging of the human brainstem. *NeuroImage* 86, 91–98. doi:10.1016/j.neuroimage.2013.07.081
- Bernier, M., Chamberland, M., Houde, J.-C., Descoteaux, M., Whittingstall, K., 2014. Using fMRI non-local means denoising to uncover activation in sub-cortical structures at 1.5 T for guided HARDI tractography. *Front. Hum. Neurosci.* 8, 715. doi:10.3389/fnhum.2014.00715

- Bosma, R.L., Stroman, P.W., 2014. Assessment of data acquisition parameters, and analysis techniques for noise reduction in spinal cord fMRI data. *Magn. Reson. Imaging* 32, 473–481. doi:10.1016/j.mri.2014.01.007
- Bouwman, C.J.C., Wilmink, J.T., Mess, W.H., Backes, W.H., 2008. Spinal cord functional MRI at 3 T: gradient echo echo-planar imaging versus turbo spin echo. *NeuroImage* 43, 288–296. doi:10.1016/j.neuroimage.2008.07.024
- Boyacıoğlu, R., Schulz, J., Koopmans, P.J., Barth, M., Norris, D.G., 2015. Improved sensitivity and specificity for resting state and task fMRI with multiband multi-echo EPI compared to multi-echo EPI at 7 T. *NeuroImage* 119, 352–361. doi:10.1016/j.neuroimage.2015.06.089
- Brooks, J., 2014. Physiological Noise Modeling and Analysis for Spinal Cord fMRI, in: Cohen-Adad, J., Wheeler-Kingshott, C. (Eds.), *Quantitative MRI of the Spinal Cord*. Academic Press, pp. 240–257.
- Brooks, J.C.W., Beckmann, C.F., Miller, K.L., Wise, R.G., Porro, C.A., Tracey, I., Jenkinson, M., 2008. Physiological noise modelling for spinal functional magnetic resonance imaging studies. *NeuroImage* 39, 680–692. doi:10.1016/j.neuroimage.2007.09.018
- Brooks, J.C.W., Kong, Y., Lee, M.C., Warnaby, C.E., Wanigasekera, V., Jenkinson, M., Tracey, I., 2012. Stimulus Site and Modality Dependence of Functional Activity within the Human Spinal Cord. *J. Neurosci.* 32, 6231–6239. doi:10.1523/JNEUROSCI.2543-11.2012
- Buades, A., Coll, B., Morel, J.M., 2005. A non-local algorithm for image denoising, in: 2005 IEEE Computer Society Conference on Computer Vision and Pattern Recognition (CVPR'05). Presented at the 2005 IEEE Computer Society Conference on Computer Vision and Pattern Recognition (CVPR'05), pp. 60–65 vol. 2. doi:10.1109/CVPR.2005.38
- Cadotte, D.W., Fehlings, M.G., 2013. Spinal cord injury: Visualizing plasticity and repair in the injured CNS. *Nat. Rev. Neurol.* 9, 546–547. doi:10.1038/nrneurol.2013.190
- Chen, J.E., Glover, G.H., 2015. BOLD fractional contribution to resting-state functional connectivity above 0.1 Hz. *NeuroImage* 107, 207–218. doi:10.1016/j.neuroimage.2014.12.012
- Chen, L.M., Mishra, A., Yang, P.-F., Wang, F., Gore, J.C., 2015. Injury alters intrinsic functional connectivity within the primate spinal cord. *Proc. Natl. Acad. Sci. U. S. A.* 112, 5991–5996. doi:10.1073/pnas.1424106112
- Cohen-Adad, J., De Leener, B., Benhamou, M., Levy, S., Touati, J., Cadotte, D., Fleet, D., Cadotte, A., Fehlings, M., Pelletier Paquette, J.P., Thong, W., Taso, M., Collins, L., Callot, V., Fonov, V., 2014. Spinal Cord Toolbox: an open-source framework for processing spinal cord MRI data. OHBM.

- Cohen-Adad, J., Gauthier, C.J., Brooks, J.C.W., Slessarev, M., Han, J., Fisher, J.A., Rossignol, S., Hoge, R.D., 2010. BOLD signal responses to controlled hypercapnia in human spinal cord. *NeuroImage* 50, 1074–1084. doi:10.1016/j.neuroimage.2009.12.122
- Cohen-Adad, J., Hoge, R.D., Leblond, H., Xie, G., Beaudoin, G., Song, A.W., Krueger, G., Doyon, J., Benali, H., Rossignol, S., 2009a. Investigations on spinal cord fMRI of cats under ketamine. *NeuroImage* 44, 328–339. doi:10.1016/j.neuroimage.2008.09.023
- Cohen-Adad, J., Levy, S., Avants, B., 2015. Slice-by-slice regularized registration for spinal cord MRI: SliceReg. ISMRM.
- Cohen-Adad, J., Rossignol, S., Hoge, 2009b. Slice-by-slice motion correction in spinal cord fMRI: SliceCorr. ISMRM.
- Cohen-Adad, J., Wald, L., 2014. Array Coils, in: Cohen-Adad, J., Wheeler-Kingshott, C. (Eds.), *Quantitative MRI of the Spinal Cord*. Academic Press, pp. 59–67.
- Cooke, F.J., Blamire, A.M., Manners, D.N., Styles, P., Rajagopalan, B., 2004. Quantitative proton magnetic resonance spectroscopy of the cervical spinal cord. *Magn. Reson. Med.* 51, 1122–1128. doi:10.1002/mrm.20084
- Coupe, P., Yger, P., Prima, S., Hellier, P., Kervrann, C., Barillot, C., 2008. An optimized blockwise nonlocal means denoising filter for 3-D magnetic resonance images. *IEEE Trans. Med. Imaging* 27, 425–441. doi:10.1109/TMI.2007.906087
- Dagli, M.S., Ingelholm, J.E., Haxby, J.V., 1999. Localization of cardiac-induced signal change in fMRI. *NeuroImage* 9, 407–415. doi:10.1006/nimg.1998.0424
- Deckers, R.H.R., van Gelderen, P., Ries, M., Barret, O., Duyn, J.H., Ikonomidou, V.N., Fukunaga, M., Glover, G.H., de Zwart, J.A., 2006. An adaptive filter for suppression of cardiac and respiratory noise in MRI time series data. *NeuroImage* 33, 1072–1081. doi:10.1016/j.neuroimage.2006.08.006
- Faull, O.K., Jenkinson, M., Ezra, M., Pattinson, K.T., 2016. Conditioned respiratory threat in the subdivisions of the human periaqueductal gray. *eLife* 5. doi:10.7554/eLife.12047
- Figley, C.R., Stroman, P.W., 2009. Development and validation of retrospective spinal cord motion time-course estimates (RESPITE) for spin-echo spinal fMRI: Improved sensitivity and specificity by means of a motion-compensating general linear model analysis. *NeuroImage* 44, 421–427. doi:10.1016/j.neuroimage.2008.08.040
- Figley, C.R., Stroman, P.W., 2007. Investigation of human cervical and upper thoracic spinal cord motion: implications for imaging spinal cord structure and function. *Magn. Reson. Med.* 58, 185–189. doi:10.1002/mrm.21260
- Finsterbusch, J., 2014. B0 Inhomogeneity and Shimming, in: Cohen-Adad, J., Wheeler-Kingshott, C. (Eds.), *Quantitative MRI of the Spinal Cord*. Academic Press, pp. 68–90.

- Finsterbusch, J., 2013. Functional neuroimaging of inner fields-of-view with 2D-selective RF excitations. *Magn. Reson. Imaging* 31, 1228–1235. doi:10.1016/j.mri.2013.03.005
- Finsterbusch, J., Eippert, F., Büchel, C., 2012. Single, slice-specific z-shim gradient pulses improve T2*-weighted imaging of the spinal cord. *NeuroImage* 59, 2307–2315. doi:10.1016/j.neuroimage.2011.09.038
- Foerster, B.R., Welsh, R.C., Feldman, E.L., 2013. 25 years of neuroimaging in amyotrophic lateral sclerosis. *Nat. Rev. Neurol.* 9, 513–524. doi:10.1038/nrneurol.2013.153
- Fradet, L., Arnoux, P.-J., Ranjeva, J.-P., Petit, Y., Callot, V., 2014. Morphometrics of the entire human spinal cord and spinal canal measured from in vivo high-resolution anatomical magnetic resonance imaging. *Spine* 39, E262–269. doi:10.1097/BRS.0000000000000125
- Fratini, M., Moraschi, M., Maraviglia, B., Giove, F., 2013. On the impact of physiological noise in spinal cord functional MRI. *J. Magn. Reson. Imaging JMRI*. doi:10.1002/jmri.24467
- Freund, P., Curt, A., Friston, K., Thompson, A., 2013. Tracking changes following spinal cord injury: insights from neuroimaging. *The Neuroscientist* 19, 116–128. doi:10.1177/1073858412449192
- Giove, F., Garreffa, G., Giulietti, G., Mangia, S., Colonnese, C., Maraviglia, B., 2004. Issues about the fMRI of the human spinal cord. *Magn. Reson. Imaging* 22, 1505–1516. doi:10.1016/j.mri.2004.10.015
- Glover, G.H., Li, T.Q., Ress, D., 2000. Image-based method for retrospective correction of physiological motion effects in fMRI: RETROICOR. *Magn. Reson. Med.* 44, 162–167.
- Griffanti, L., Douaud, G., Bijsterbosch, J., Evangelisti, S., Alfaro-Almagro, F., Glasser, M.F., Duff, E.P., Fitzgibbon, S., Westphal, R., Carone, D., Beckmann, C., Smith, S.M. Submitted. How to hand-classify fMRI ICA noise components. *NeuroImage*.
- Griswold, M.A., Jakob, P.M., Heidemann, R.M., Nittka, M., Jellus, V., Wang, J., Kiefer, B., Haase, A., 2002. Generalized autocalibrating partially parallel acquisitions (GRAPPA). *Magn. Reson. Med.* 47, 1202–1210. doi:10.1002/mrm.10171
- Guimaraes, A.R., Melcher, J.R., Talavage, T.M., Baker, J.R., Ledden, P., Rosen, B.R., Kiang, N.Y., Fullerton, B.C., Weisskoff, R.M., 1998. Imaging subcortical auditory activity in humans. *Hum. Brain Mapp.* 6, 33–41.
- Hallquist, M.N., Hwang, K., Luna, B., 2013. The nuisance of nuisance regression: spectral misspecification in a common approach to resting-state fMRI preprocessing reintroduces noise and obscures functional connectivity. *NeuroImage* 82, 208–225. doi:10.1016/j.neuroimage.2013.05.116

- Henry-Feugeas, M.C., Idy-Peretti, I., Baledent, O., Poncelet-Didon, A., Zannoli, G., Bittoun, J., Schouman-Claeys, E., 2000. Origin of subarachnoid cerebrospinal fluid pulsations: a phase-contrast MR analysis. *Magn. Reson. Imaging* 18, 387–395.
- Huettel, S.A., Song, A.W., McCarthy, G. 2014. *Functional magnetic resonance imaging*. Sinauer Associates.
- Hutton, C., Josephs, O., Stadler, J., Featherstone, E., Reid, A., Speck, O., Bernarding, J., Weiskopf, N., 2011. The impact of physiological noise correction on fMRI at 7T. *NeuroImage* 57, 101–112. doi:10.1016/j.neuroimage.2011.04.018
- Hu, X., Le, T.H., Parrish, T., Erhard, P., 1995. Retrospective estimation and correction of physiological fluctuation in functional MRI. *Magn. Reson. Med.* 34, 201–212.
- Jenkinson, M., Bannister, P., Brady, M., Smith, S., 2002. Improved optimization for the robust and accurate linear registration and motion correction of brain images. *NeuroImage* 17, 825–841.
- Johanssen, H.C., Helmchen, F. 2013. Two-photon imaging of spinal cord cellular networks. *Exp. Neurol.* 242, 18–26.
- Jones, T.B., Bandettini, P.A., Birn, R.M., 2008. Integration of motion correction and physiological noise regression in fMRI. *NeuroImage* 42, 582–590. doi:10.1016/j.neuroimage.2008.05.019
- Kelly, R.E., Alexopoulos, G.S., Wang, Z., Gunning, F.M., Murphy, C.F., Morimoto, S.S., Kanellopoulos, D., Jia, Z., Lim, K.O., Hoptman, M.J., 2010. Visual inspection of independent components: defining a procedure for artifact removal from fMRI data. *J. Neurosci. Methods* 189, 233–245. doi:10.1016/j.jneumeth.2010.03.028
- Ko, H.-Y., Park, J.H., Shin, Y.B., Baek, S.Y., 2004. Gross quantitative measurements of spinal cord segments in human. *Spinal Cord* 42, 35–40. doi:10.1038/sj.sc.3101538
- Kong, Y., Eippert, F., Beckmann, C.F., Andersson, J., Finsterbusch, J., Büchel, C., Tracey, I., Brooks, J.C.W., 2014. Intrinsically organized resting state networks in the human spinal cord. *Proc. Natl. Acad. Sci. U. S. A.* doi:10.1073/pnas.1414293111
- Kong, Y., Jenkinson, M., Andersson, J., Tracey, I., Brooks, J.C.W., 2012. Assessment of physiological noise modelling methods for functional imaging of the spinal cord. *NeuroImage* 60, 1538–1549. doi:10.1016/j.neuroimage.2011.11.077
- Kundu, P., Inati, S.J., Evans, J.W., Luh, W.-M., Bandettini, P.A., 2012. Differentiating BOLD and non-BOLD signals in fMRI time series using multi-echo EPI. *NeuroImage* 60, 1759–1770. doi:10.1016/j.neuroimage.2011.12.028
- Lawrence, J., Stroman, P.W., Bascaramurty, S., Jordan, L.M., Malisza, K.L., 2004. Correlation of functional activation in the rat spinal cord with neuronal activation detected by immunohistochemistry. *NeuroImage* 22, 1802–1807. doi:10.1016/j.neuroimage.2004.04.001
- Lee, G., Jordan, C., Tiet, P., Ruiz, C., McCormick, J., Phuong, K., Hargreaves, B., Conolly, S., 2015. Improved frequency selective fat suppression in the posterior neck

with tissue susceptibility matched pyrolytic graphite foam. *J. Magn. Reson. Imaging* 41, 684–693. doi:10.1002/jmri.24581

Lilja, J., Endo, T., Hofstetter, C., Westman, E., Young, J., Olson, L., Spenger, C., 2006. Blood oxygenation level-dependent visualization of synaptic relay stations of sensory pathways along the neuroaxis in response to graded sensory stimulation of a limb. *J. Neurosci.* 26, 6330–6336. doi:10.1523/JNEUROSCI.0626-06.2006

Li, L., Miller, K.L., Jezzard, P., 2012. DANTE-prepared pulse trains: a novel approach to motion-sensitized and motion-suppressed quantitative magnetic resonance imaging. *Magn. Reson. Med.* 68, 1423–1438. doi:10.1002/mrm.24142

Malinen, S., Schürmann, M., Hlushchuk, Y., Forss, N., Hari, R., 2006. Improved differentiation of tactile activations in human secondary somatosensory cortex and thalamus using cardiac-triggered fMRI. *Exp. Brain Res.* 174, 297–303. doi:10.1007/s00221-006-0465-z

Manjón, J.V., Coupé, P., Martí-Bonmatí, L., Collins, D.L., Robles, M., 2010. Adaptive non-local means denoising of MR images with spatially varying noise levels. *J. Magn. Reson. Imaging* 31, 192–203. doi:10.1002/jmri.22003

Moher Alsady, T., Blessing, E.M., Beissner, F., 2016. MICA-A toolbox for masked independent component analysis of fMRI data. *Hum. Brain Mapp.* doi:10.1002/hbm.23258

Montgomery, K.L., Iyer, S.M., Christensen, A.J., Deisseroth, K., Delp, S.L., 2016. Beyond the brain: Optogenetic control in the spinal cord and peripheral nervous system. *Sci. Transl. Med.* 8, 337rv5. doi:10.1126/scitranslmed.aad7577

Murphy, K., Birn, R.M., Bandettini, P.A., 2013. Resting-state fMRI confounds and cleanup. *NeuroImage* 80, 349–359. doi:10.1016/j.neuroimage.2013.04.001

Muschelli, J., Nebel, M.B., Caffo, B.S., Barber, A.D., Pekar, J.J., Mostofsky, S.H., 2014. Reduction of motion-related artifacts in resting state fMRI using aCompCor. *NeuroImage* 96, 22–35. doi:10.1016/j.neuroimage.2014.03.028

Niazy, R.K., Xie, J., Miller, K., Beckmann, C.F., Smith, S.M., 2011. Spectral characteristics of resting state networks. *Prog. Brain Res.* 193, 259–276. doi:10.1016/B978-0-444-53839-0.00017-X

O'Connell, J.E.A., 1943. The Vascular Factor In Intracranial Pressure and the Maintenance of the Cerebrospinal Fluid Circulation. *Brain* 66, 204–228. doi:10.1093/brain/66.3.204

Parrish, T.B., Gitelman, D.R., LaBar, K.S., Mesulam, M.M., 2000. Impact of signal-to-noise on functional MRI. *Magn. Reson. Med.* 44, 925–932.

Perlberg, V., Bellec, P., Anton, J.-L., Péligrini-Issac, M., Doyon, J., Benali, H., 2007. CORSICA: correction of structured noise in fMRI by automatic identification of ICA components. *Magn. Reson. Imaging* 25, 35–46. doi:10.1016/j.mri.2006.09.042

- Piché, M., Cohen-Adad, J., Nejad, M.K., Perlberg, V., Xie, G., Beaudoin, G., Benali, H., Rainville, P., 2009. Characterization of cardiac-related noise in fMRI of the cervical spinal cord. *Magn. Reson. Imaging* 27, 300–310. doi:10.1016/j.mri.2008.07.019
- Poldrack, R.A., Mumford, J.A., Nichols, T.E. 2011. *Handbook of functional MRI data analysis*. Cambridge University Press.
- Pórszász, R., Beckmann, N., Bruttel, K., Urban, L., Rudin, M., 1997. Signal changes in the spinal cord of the rat after injection of formalin into the hindpaw: characterization using functional magnetic resonance imaging. *Proc. Natl. Acad. Sci. U. S. A.* 94, 5034–5039.
- Power, J.D., Schlaggar, B.L., Petersen, S.E., 2015. Recent progress and outstanding issues in motion correction in resting state fMRI. *NeuroImage* 105, 536–551. doi:10.1016/j.neuroimage.2014.10.044
- Pruessmann, K.P., Weiger, M., Scheidegger, M.B., Boesiger, P., 1999. SENSE: sensitivity encoding for fast MRI. *Magn. Reson. Med.* 42, 952–962.
- Pruim, R.H.R., Mennes, M., Buitelaar, J.K., Beckmann, C.F., 2015a. Evaluation of ICA-AROMA and alternative strategies for motion artifact removal in resting state fMRI. *NeuroImage*. doi:10.1016/j.neuroimage.2015.02.063
- Pruim, R.H.R., Mennes, M., van Rooij, D., Llera, A., Buitelaar, J.K., Beckmann, C.F., 2015b. ICA-AROMA: A robust ICA-based strategy for removing motion artifacts from fMRI data. *NeuroImage*. doi:10.1016/j.neuroimage.2015.02.064
- Purdon, P.L., Weisskoff, R.M., 1998. Effect of temporal autocorrelation due to physiological noise and stimulus paradigm on voxel-level false-positive rates in fMRI. *Hum. Brain Mapp.* 6, 239–249.
- Raj, D., Anderson, A.W., Gore, J.C., 2001. Respiratory effects in human functional magnetic resonance imaging due to bulk susceptibility changes. *Phys. Med. Biol.* 46, 3331–3340.
- Salimi-Khorshidi, G., Douaud, G., Beckmann, C.F., Glasser, M.F., Griffanti, L., Smith, S.M., 2014. Automatic denoising of functional MRI data: combining independent component analysis and hierarchical fusion of classifiers. *NeuroImage* 90, 449–468. doi:10.1016/j.neuroimage.2013.11.046
- San Emeterio Nateras, O., Yu, F., Muir, E.R., Bazan, C., Franklin, C.G., Li, W., Li, J., Lancaster, J.L., Duong, T.Q., 2016. Intrinsic Resting-State Functional Connectivity in the Human Spinal Cord at 3.0 T. *Radiology* 279, 262–268. doi:10.1148/radiol.2015150768
- Saritas, E., Holdsworth, S., Bammer, R., 2014. Susceptibility Artefacts, in: Cohen-Adad, J., Wheeler-Kingshott, C. (Eds.), *Quantitative MRI of the Spinal Cord*. Academic Press, pp. 91–105.
- Schroth, G., Klose, U., 1992. Cerebrospinal fluid flow. I. Physiology of cardiac-related pulsation. *Neuroradiology* 35, 1–9.

- Shmuel, A., Yacoub, E., Chaimow, D., Logothetis, N.K., Ugurbil, K., 2007. Spatio-temporal point-spread function of fMRI signal in human gray matter at 7 Tesla. *NeuroImage* 35, 539–552. doi:10.1016/j.neuroimage.2006.12.030
- Silverdale, M., 2015. Spinal cord: internal organization, in: Standring, S. (Ed.), *Gray's Anatomy: The Anatomical Basis of Clinical Practice*.
- Stroman, P.W., 2006. Discrimination of errors from neuronal activity in functional MRI of the human spinal cord by means of general linear model analysis. *Magn. Reson. Med.* 56, 452–456. doi:10.1002/mrm.20966
- Stroman, P.W., 2005. Magnetic resonance imaging of neuronal function in the spinal cord: spinal FMRI. *Clin. Med. Res.* 3, 146–156.
- Stroman, P.W., Nance, P.W., Ryner, L.N., 1999. BOLD MRI of the human cervical spinal cord at 3 tesla. *Magn. Reson. Med.* 42, 571–576.
- Stroman, P.W., Wheeler-Kingshott, C., Bacon, M., Schwab, J.M., Bosma, R., Brooks, J., Cadotte, D., Carlstedt, T., Ciccarelli, O., Cohen-Adad, J., Curt, A., Evangelou, N., Fehlings, M.G., Filippi, M., Kelley, B.J., Kollias, S., Mackay, A., Porro, C.A., Smith, S., Strittmatter, S.M., Summers, P., Tracey, I., 2014. The current state-of-the-art of spinal cord imaging: methods. *NeuroImage* 84, 1070–1081. doi:10.1016/j.neuroimage.2013.04.124
- Summers, P.E., Iannetti, G.D., Porro, C.A., 2010. Functional exploration of the human spinal cord during voluntary movement and somatosensory stimulation. *Magn. Reson. Imaging* 28, 1216–1224. doi:10.1016/j.mri.2010.05.001
- Summers, P., Staempfli, P., Jaermann, T., Kwiecinski, S., Kollias, S., 2006. A preliminary study of the effects of trigger timing on diffusion tensor imaging of the human spinal cord. *AJNR Am. J. Neuroradiol.* 27, 1952–1961.
- Thron, A., 2016. *Vascular Anatomy of the Spinal Cord*, 2nd ed. Springer.
- Triantafyllou, C., Hoge, R.D., Krueger, G., Wiggins, C.J., Potthast, A., Wiggins, G.C., Wald, L.L., 2005. Comparison of physiological noise at 1.5 T, 3 T and 7 T and optimization of fMRI acquisition parameters. *NeuroImage* 26, 243–250. doi:10.1016/j.neuroimage.2005.01.007
- Vahdat, S., Lungu, O., Cohen-Adad, J., Marchand-Pauvert, V., Benali, H., Doyon, J., 2015. Simultaneous Brain-Cervical Cord fMRI Reveals Intrinsic Spinal Cord Plasticity during Motor Sequence Learning. *PLoS Biol.* 13, e1002186. doi:10.1371/journal.pbio.1002186
- van Gelderen, P., de Zwart, J.A., Starewicz, P., Hinks, R.S., Duyn, J.H., 2007. Real-time shimming to compensate for respiration-induced B0 fluctuations. *Magn. Reson. Med.* 57, 362–368. doi:10.1002/mrm.21136
- Verma, T., Cohen-Adad, J., 2014. Effect of respiration on the B0 field in the human spinal cord at 3T. *Magn. Reson. Med.* 72, 1629–1636. doi:10.1002/mrm.25075

- Weber, K.A., Chen, Y., Wang, X., Kahnt, T., Parrish, T.B., 2016. Lateralization of cervical spinal cord activity during an isometric upper extremity motor task with functional magnetic resonance imaging. *NeuroImage* 125, 233–243. doi:10.1016/j.neuroimage.2015.10.014
- Weber, K.A., Chen, Y., Wang, X., Parrish, T.B., 2014. Choice of Motion Correction Method Affects Spinal Cord fMRI Results. *OHBM*.
- Welvaert, M., Rosseel, Y. 2013. On the definition of signal-to-noise ratio and contrast-to-noise ratio for fMRI data. *PLoS ONE* 11, e77089.
- Wheeler-Kingshott, C.A., Stroman, P.W., Schwab, J.M., Bacon, M., Bosma, R., Brooks, J., Cadotte, D.W., Carlstedt, T., Ciccarelli, O., Cohen-Adad, J., Curt, A., Evangelou, N., Fehlings, M.G., Filippi, M., Kelley, B.J., Kollias, S., Mackay, A., Porro, C.A., Smith, S., Strittmatter, S.M., Summers, P., Thompson, A.J., Tracey, I., 2014. The current state-of-the-art of spinal cord imaging: applications. *NeuroImage* 84, 1082–1093. doi:10.1016/j.neuroimage.2013.07.014
- Wilm, B.J., Svensson, J., Henning, A., Pruessmann, K.P., Boesiger, P., Kollias, S.S., 2007. Reduced field-of-view MRI using outer volume suppression for spinal cord diffusion imaging. *Magn. Reson. Med.* 57, 625–630. doi:10.1002/mrm.21167
- Wise, R.G., Ide, K., Poulin, M.J., Tracey, I., 2004. Resting fluctuations in arterial carbon dioxide induce significant low frequency variations in BOLD signal. *NeuroImage* 21, 1652–1664. doi:10.1016/j.neuroimage.2003.11.025
- Woolf, C.J., Salter, M.W., 2000. Neuronal plasticity: increasing the gain in pain. *Science* 288, 1765–1769.
- Xie, G., Piché, M., Khoshejad, M., Perlberg, V., Chen, J.-I., Hoge, R.D., Benali, H., Rossignol, S., Rainville, P., Cohen-Adad, J., 2012. Reduction of physiological noise with independent component analysis improves the detection of nociceptive responses with fMRI of the human spinal cord. *NeuroImage*. doi:10.1016/j.neuroimage.2012.06.057
- Yang, P.-F., Wang, F., Chen, L.M., 2015. Differential fMRI Activation Patterns to Noxious Heat and Tactile Stimuli in the Primate Spinal Cord. *J. Neurosci.* 35, 10493–10502. doi:10.1523/JNEUROSCI.0583-15.2015
- Yoshizawa, T., Nose, T., Moore, G.J., Sillerud, L.O., 1996. Functional magnetic resonance imaging of motor activation in the human cervical spinal cord. *NeuroImage* 4, 174–182. doi:10.1006/nimg.1996.0068
- Zarahn, E., Aguirre, G.K., D'Esposito, M., 1997. Empirical analyses of BOLD fMRI statistics. I. Spatially unsmoothed data collected under null-hypothesis conditions. *NeuroImage* 5, 179–197.
- Zhang, L., Kholmovski, E.G., Guo, J., Choi, S.-E.K., Morrell, G.R., Parker, D.L., 2009. HASTE sequence with parallel acquisition and T2 decay compensation: application to

carotid artery imaging. *Magn. Reson. Imaging* 27, 13–22. doi:10.1016/j.mri.2008.05.009

Zhao, F., Williams, M., Welsh, D.C., Meng, X., Ritter, A., Abbadie, C., Cook, J.J., Reicin, A.S., Hargreaves, R., Williams, D.S., 2009. fMRI investigation of the effect of local and systemic lidocaine on noxious electrical stimulation-induced activation in spinal cord. *Pain* 145, 110–119. doi:10.1016/j.pain.2009.05.026

Zhao, W., Cohen-Adad, J., Polimeni, J.R., Keil, B., Guerin, B., Setsompop, K., Serano, P., Mareyam, A., Hoecht, P., Wald, L.L., 2014. Nineteen-channel receive array and four-channel transmit array coil for cervical spinal cord imaging at 7T. *Magn. Reson. Med.* 72, 291–300. doi:10.1002/mrm.24911

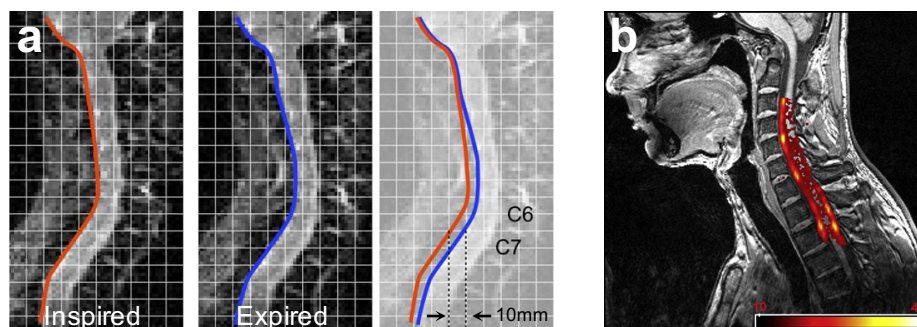


Figure 1. Examples of physiological noise. a) Sagittal sections through the spinal cord during an inspired (left) and an expired state (middle). The panel on the right shows that there is a cord displacement of almost 10mm (corresponding approximately to the anterior-posterior diameter of the cord) between the two states, demonstrating the importance of addressing respiratory sources of physiological noise (Verma & Cohen-Adad, 2014). **b)** A sagittal section through the spinal cord with a coloured overlay of signal changes within the cardiac frequency (of critically sampled fMRI data) in terms of percent signal change. The highest signal changes are observed in the CSF and at the edge of the cord, but clearly extend into the cord as well, demonstrating the importance of addressing cardiac sources of physiological noise (Piche et al., 2009). With permission from a) John Wiley and Sons and b) Elsevier.

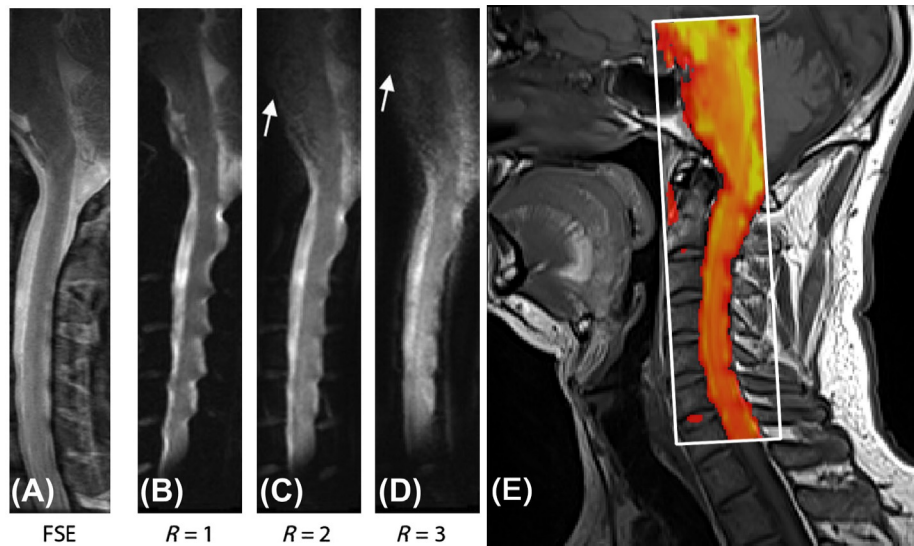


Figure 2. Addressing image distortion. Adapted from Saritas et al. (2014). Cervical spine images acquired using a four channel spine array coil using a matrix size = 192 x 192 and FOV = 18 x 9 cm (with phase-encoding in the A/P direction). **A)** T2-weighted fast spin-echo (FSE) image is given for anatomical reference. Standard single-shot EPI with **B)** no acceleration ($R=1$), **C)** $R = 2$ giving a twofold reduction in geometric distortion, and **D)** $R = 3$ giving a threefold reduction in geometric distortion. Because of the shorter trajectory and g-factor noise present in (C–D), the SNR is reduced overall. Especially the pons area experiences a significant SNR reduction, due to the diminishing coil sensitivity profiles in the A/P direction (white arrow). The decreased image quality with $R = 3$ suggests that $R = 2$ is probably the upper acceleration limit for this spine array coil. An alternative approach to minimising susceptibility induced image distortion, whilst avoiding G-factor penalty, is to use selective excitation of an inner field of view. The ZoomIT pulse sequence (available on Siemens scanners with parallel-transmit capabilities) was utilised to acquire the axial fMRI data in **E)**, which were resliced, shaded red-yellow and superimposed on a sagittal T1-weighted spin-echo anatomical reference. The selected region was encoded with 96 x 36 k-space lines, with TE/TR = 30/3000ms, and 36 slices covering from T1 to midbrain on a Siemens Prisma 3T system with a 64-channel head and neck coil. Good agreement between the location of the spinal cord on fMRI data and the underlying anatomical reference can be seen. With permission from Elsevier.

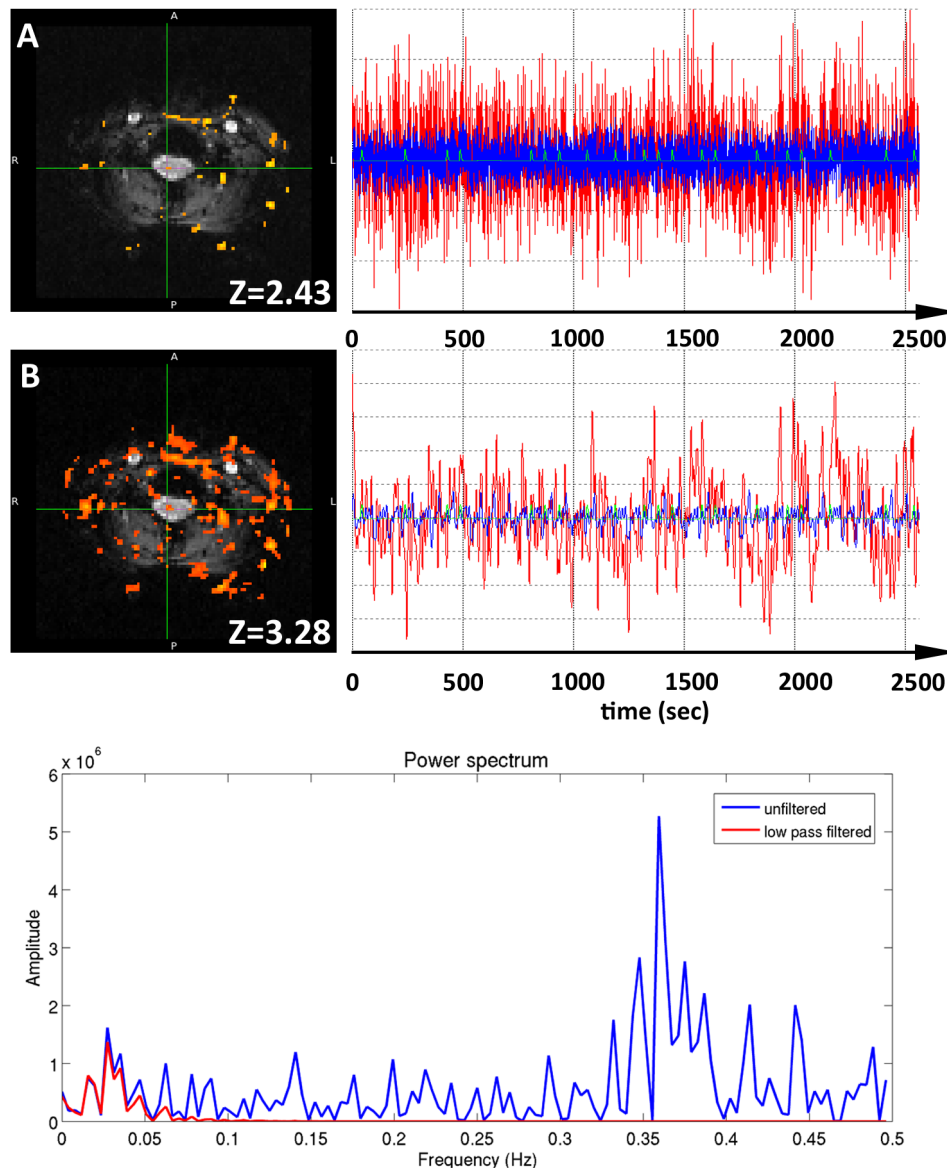


Figure 3. Illustration of the undesired effects of low-pass filtering. Data are from a single subject's spinal fMRI experiment, with the time-series data and resultant statistical maps (threshold $Z > 2.3$, $p < 0.01$; Brooks, 2014). The only difference between A and B is that the latter had a low-pass filter applied (cut-off 0.1Hz) prior to GLM estimation. It is clear that the time-series are temporally smoothed by this procedure – and the effect on the power spectrum is shown below. The action of the low-pass filter is to remove 80% of the noise associated with this experiment, increasing the Z-score of the “activated” voxels in the cord (if not adjusting for loss of degrees of freedom in the model), but more importantly dramatically increasing the false-positive rate in the non-neuronal tissue of the neck (e.g. in the trachea and vertebral bodies). It should be clear that even the application of a more modest low-pass filter (e.g. cut-off 0.3Hz) would still lead to artificial inflation of statistics. The reality is that the data (as acquired) are the time-series in A, and thus the confidence of detecting activation is lower than if the acquired time-series data were as in B. With permission from Elsevier.

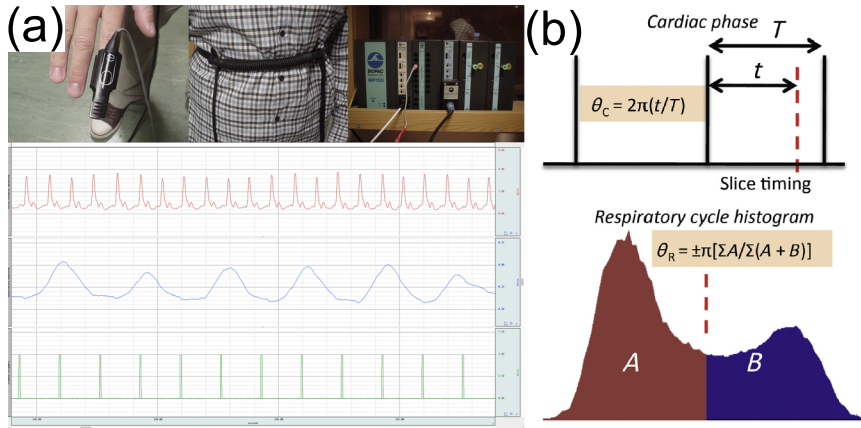


Figure 4. Model-based physiological noise correction. **a)** A typical set-up for acquisition of physiological traces, which are shown below (Brooks, 2014). From left to right, the pulse-oximeter (also known as photoplethysmograph) is used to sample the cardiac cycle (first trace), the respiratory bellows is used to record chest wall diameter (second trace), a surrogate for the volume of air in the lungs. The physiological traces and scanner volume trigger (third trace) are stored on a commercially available analog-to-digital converter / data logging device - here the BIOPAC MP150 (Goleta, USA). **b)** An illustration of phase calculation based on recorded physiological waveforms (Kong et al., 2012). The cardiac phase (“ θ_C ”) associated with each image slice is assigned by measuring the timing of slice acquisition (“ t ”) relative to the adjacent peaks in the pulse oximeter trace (“ T ”; corresponding to the ECG R-waves). Respiratory phase (“ θ_R ”) is defined by using a histogram-equalized transfer function (see main text), and is the ratio of the sum of respiratory bellows values up to the value at the time of slice acquisition (“ A ”), taken from the respiratory histogram, divided by the sum of all respiratory bellows values (“ $A+B$ ”). The sign of the respiratory phase is dependent on whether the lungs were inflating or deflating at the time of slice acquisition. With permission from Elsevier.